The Depths of Magma Chambers under the Galapagos Ridge

Presented in Partial Fulfillment of the Requirements for Graduation
with a Bachelor of Science in Geological Sciences in the
undergraduate colleges of The Ohio State University

by

Emily V. England

The Ohio State University
August 2008

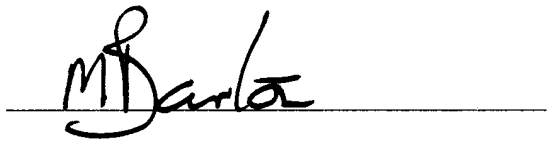

Dr. Michael Barton
Advisor

Table of Contents

ACKNOWLEDGEMENTS

I would like to give thanks to the following people for helping me with my research on the Galapagos ridge while at The Ohio State University: my research advisor Dr. Michael Barton who suggested this project and mentored me along the way, Dr. Wendy Panero for her time and conversation, graduate student Daniel Kelley, and classmate Jameson “Dino” Scott.

I would also like to acknowledge the entire Geological Sciences Department at OSU. I have been thoroughly pleased with my education and believe that I have found a field that I will enjoy and pursue for the rest of my life.

And of course I thank my parents and family for more than words can say.

ABSTRACT

The Galapagos Ridge System is one of the most unique ridges on the Earth. Galapagos spreads at an intermediate rate of 47 to ~63 mm/yr (Canales et al., 2002). We speculate that spreading rate may influence the depth of partial crystallization and the structure of magma plumbing systems beneath ridges. To constrain the depth at which partial crystallization of magmas occurs beneath the GSC, we have used a method to calculate the pressure of crystallization that is more accurate and reliable than similar methods, such as that described by Claude Herzberg (2004, Journal of Petrology). The method involves calculating the pressure at which a liquid, represented by volcanic glass, is chemically in equilibrium with olivine, plagioclase, and augite. Our data set is comprised of analyses of volcanic glass collected on scientific cruises along the Galapagos ridge. These analyses were downloaded from the RIDGE data base which is maintained by Lamont- Doherty Earth Observatory. Filtering of the analyses was necessary to exclude glasses that were not in equilibrium with olivine, plagioclase, and augite. The 1,110 remaining glasses were then divided into twelve groups based on longitude. Results indicate that Galapagos magmas crystallize over a range of pressure from 0.07- 9.36 kBar, equivalent to 0.23 to 32.94 km depth, but that most crystallization occurs at 2.99 ± 1.92 kBar, or a depth of 10 ± 2.5 km. Some of these chambers are probably located just beneath the crust in the uppermost mantle. This range of depth suggests that the magma plumbing system is complex and is likely composed of multiple, stacked chambers that are interconnected by dikes. In fact, we are finding evidence for magma chambers at two different depths on the more western end of the ridge, whereas

there seems to be evidence for a single magma chamber on the more eastern end of the ridge. Emily Klein and co-workers have shown that Na_8 (Na normalized to 8.0 wt % MgO) is a measure of crustal thickness with low values indicating higher mantle temperatures and greater degrees of melting. Overall, we find that Na_8 decreases with increasing depth, and is exceptionally low near 92º W which lies on the same latitude as the Galapagos hotspot. Implications for the interpretation of the Galapagos magma plumbing system include the possible influence of the Galapagos hotspot as well as transform faults near the western end of the ridge on magma plumbing systems.

INTRODUCTION

This is one of the first attempts to try to constrain the depths of magma chambers using geochemical methods under the Galapagos Ridge, or Galapagos Spreading Center (GSC). There have been other studies to constrain the depths of chambers under Iceland and the Reykjanes ridge such as Kelley and Barton, 2008. In general, the importance of studying the depths of magma chambers can be explained by three main reasons. First, magma chamber depth is closely related to magma evolution and at what depth magma crystallizes since phase relationships and melt composition varies as a function of pressure (eg. Grove et al. 1992; Yang et al. 1996). Second, the depth of magma chambers will also help us understand the geothermal gradient under the Galapagos ridge, which is reflected in variations in density and seismic velocity. Lastly, we would like to better understand the relationship between spreading rate, crustal thickness and magma chamber depth. This is especially interesting as the GSC has a fast spreading western portion (~47mm/yr) and a slower spreading eastern portion (~63mm/yr). If we can get a concise understanding of how spreading rate and crustal thickness relate to chamber depth at the Galapagos ridge, we may be able to predict chamber depths based on known spreading rates and crustal thickness at other ridges. This could further our knowledge of the mechanisms and related structure of mid-ocean ridges worldwide.

Methods that have been used to estimate magma chamber depths involve geodetic and geophysical techniques. Geophysical techniques include seismic, gravity, and magnetic measurements which give information about crustal thickness, crust/mantle density, buoyancy, and temperature. Geodetic techniques include ground or satellite GPS

measurements that can detect slight differences in vertical elevation or surface tilt. For example, Sturkell at el. (2006) have used geodetic techniques to determine chamber depth under Iceland that often agree with depths estimated using geophysical techniques. Canales et al, 2002, have described the maximum thickness of the crust along the GSC to be ~8 km at the eastern end (91º W) while the minimum thickness is ~5.6 km at the western end (97º W). Despite these previous studies geodetic techniques do not always agree with geophysical techniques especially when locating chambers beneath active volcanoes (Soosalu & Einarsson, 2004). Petrologic methods, however, allow the depths of magma chambers beneath active and inactive volcanic centers to be determined.

In this paper, petrologic techniques involve the analysis of volcanic glass to determine the pressure, and hence the depth, of crystallization. Pressures of crystallization are determined from experimentally established phase equilibrium constraints using a method similar to the one described by Yang et al. (1996). As stated before, the samples we use to determine pressure are volcanic glasses, which represent pre-eruptive liquid compositions. These pressures were then divided in 12 localities that span the east-west oriented GSC, based on the longitude at which the glasses were acquired, so that we may describe the characteristics of magma chambers at each location. Later, we discuss the implications of the results for the relation of spreading rate to chamber depth, geothermal gradient, and magma evolution.

BACKGROUND

The Galapagos Archipelago, which consists of 14 main islands and several rocky islets, lies along the equator, roughly 600 miles off the coast of South America (McBirney, 1969). The islands were never connected to South or Central America. They are thought to be a product of the Galapagos hotspot, or mantle plume, which is now located under the present day Fernandina Island on the Nazca plate. Although this plume does not create such a simple linear chain of islands such as the Hawaiian plume, the Galapagos Islands do get older in age as you move to the south-southeast (Espanola Island being the oldest). Two types of volcanoes occur on the Galapagos Islands which are separated by a large transform fault, known as the Wolf-Darwin lineament (WDL), located at 91˚W. This fracture zone separates oceanic crust and lithosphere of different ages (White, 1997). To the west the lithosphere is older and thicker and therefore able to support large volcanoes with deep calderas on the islands of Fernandina and Isabella. To the east the younger, thin lithosphere can only support small shield volcanoes with gentler slopes.

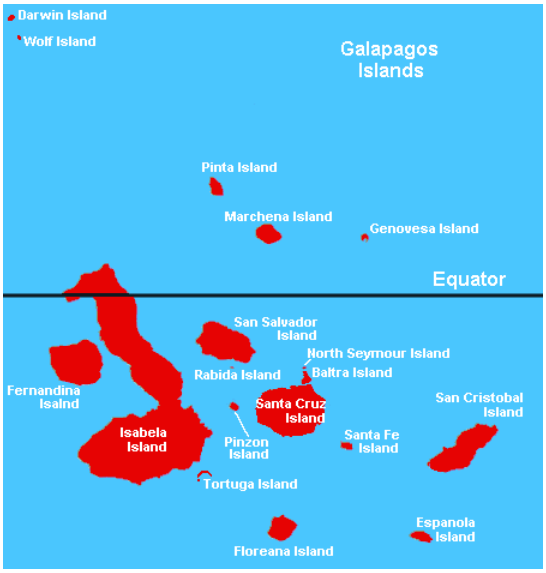

Figure 1. Map of the Galapagos Islands in relation to the equator. (http://www.ecuadortouristboard.com/regions/galapagos/images/map_galapagos_a450w.gif)

The Galapagos Spreading Center runs westward along the latitude 2˚N from Darwin (Culpepper) Island at the northern end of the archipelago until it cuts and offsets the crest of the East Pacific Rise and then continues beyond. Its total length is approximately 1600 miles (White, 2007). The GSC separates the Cocos plate to the north from the Nazca plate to the south. At 98º W the ridge opens at 47 mm/yr while at 91º W the ridge opens at 63 mm/yr (Canales et al., 2002). At 91º W the GSC lies ~200 km north of the Galapagos Archipelago, the western end of which marks the probable center of the Galapagos mantle plume (White et al., 1993; Toomey et al., 2001). The hot spot has a strong influence on the GSC. This can be seen in along axis variations in bathymetry and gravity (Ito and Lin, 1995a), axial geomorphology (Canales et al., 2007), in the chemical and isotopic composition of GSC basalts (Schilling et al., 1976; Fisk et al., 1982; Verma and Schilling, 1982; Verma et al., 1983), and in the long history of rift propagation along the GSC (Hey, 1977; Wilson and Hey, 1995). For example, approaching the Galapagos Spreading Center from the west the hot spot swell shoals by ~700 m, and the mantle Bouguer gravity (MBA) decreases by ~60 mGal. Chemically, another example of the influence of the Galapagos hotspot on the GSC is its affect on the concentration of incompatible elements in magma. The hotspot is causing excess mantle temperatures of ~30º C near the ridge, which creates more melt (Canales et al., 2002). Incompatible elements preferentially enter into melt; therefore their concentration is high at low degrees of melting and low at high degrees of melting with the dilution of more compatible elements (Klein, 1987).

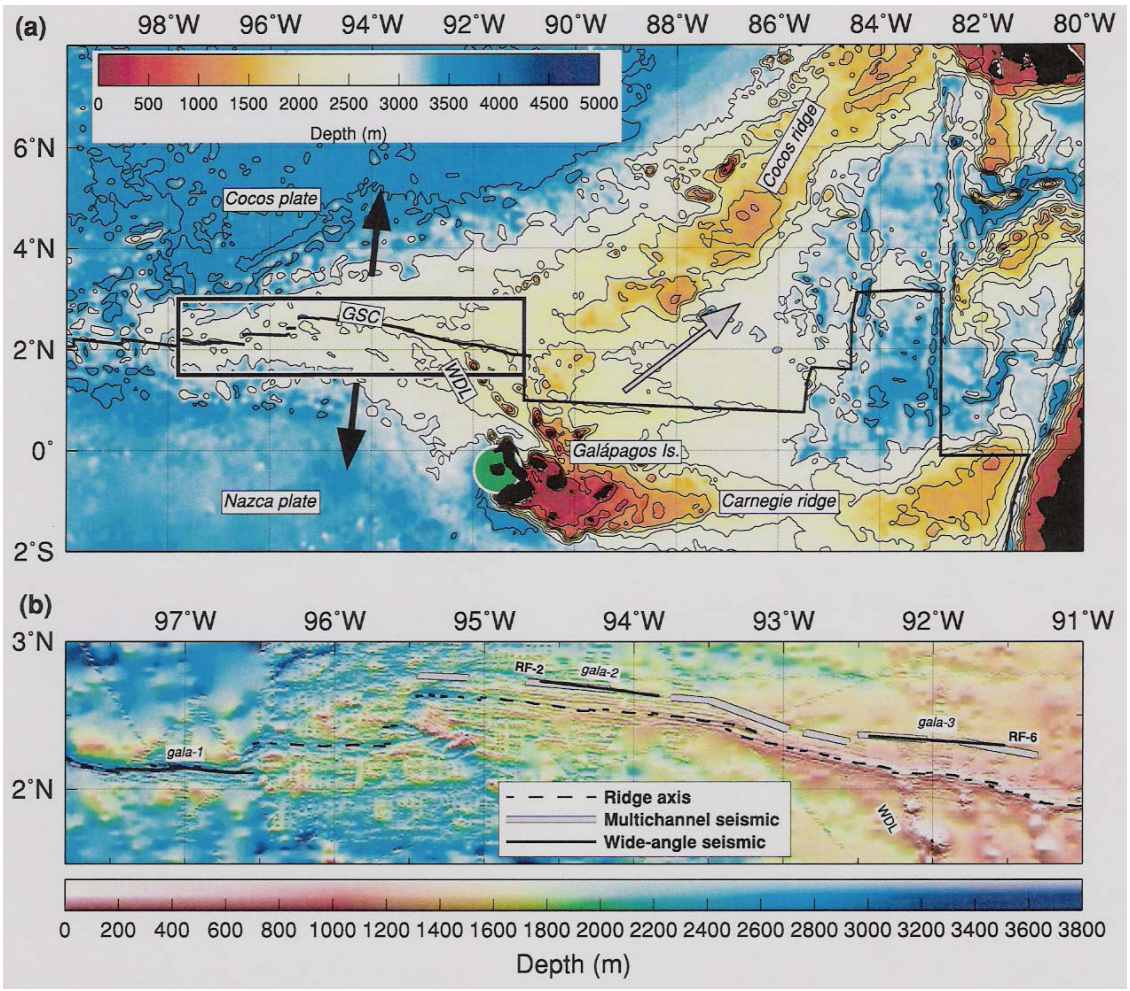

Figure 2. Area of study. Bathymetry Map of the Galapagos Region. GSC is the Galapagos Spreading Center and WDL is the Wolf-Darwin lineament. The green circle represents the present location of the Galapagos hotspot beneath Fernandina. Black arrows show the seafloor spreading direction and grey arrows indicate the migration of the ridge. Contours every 500 m. (Canales et al, 2002)

METHODS

In order to find the pressure of crystallization for 1110 glass samples we used a method that is based on comparing the compositions of erupted melts with compositions of liquid magma that lie along well defined pressure (P) dependant phase boundaries. Glasses formed from liquid in equilibrium with *ol*, *plag*, and *cpx* should have compositions that lie exactly on the cotectic at the pressure of crystallization (Kelley and Barton, 2008). Scientists such as O'Hara (1968) and Grove et al. (1992) have experimentally determined the effect of pressure on liquids lying along the olivine (*ol*)-plagioclase (*plag*)- clinopyroxene (*cpx*) cotectic boundary. To see the effect pressure has on the *ol-plag-cpx* cotectic boundary we had to recast melt compositions into normative mineral components and project phase relationships onto the pseudoternary planes in the system CaO- MgO- Al_2O_3- SiO_2. Projection of phase relationships from *plag* onto the plane *ol-plag-cpx* using the recalculation procedure of Walker et al. (1979) clearly show the shift of the *ol-plag-cpx* cotectic towards *ol* with increasing P (Fig. 4).

The shift of the *ol-plag-cpx* cotectic towards *ol* and *plag* reflects the different pressure dependencies of *cpx-liq*, *ol-liq*, and *plag-liq* equilibria, and results in decreasing CaO and increasing MgO and Al_2O_3 contents of melts with increasing P (Kelley and Barton, 2008). Several scientists have proposed models to quantitatively estimate the crystallization pressure of such relationships, but we have decided to modify and use the method described by Yang et al. (1996), who present equations which describe the composition of liquids along the *ol-plag-cpx* cotectic as a function of P and T.

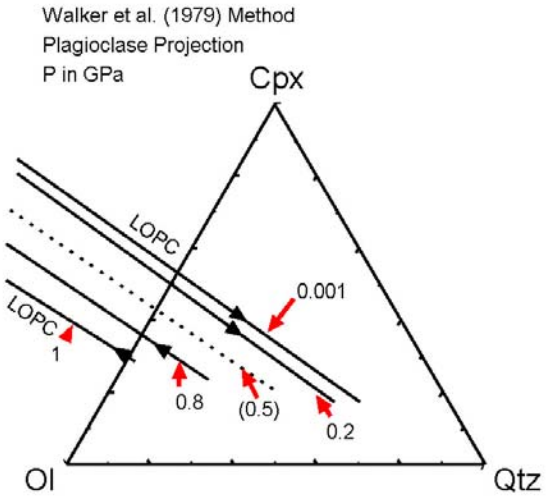

Figure 4. Position of the ol-plag-cpx cotectic at different pressures projected from plagioclase onto the pseudoternary plane Ol-Cpx-Qtz using the method described by Walker et al. (1979). Pressures of cotectic given in GPa. Locations of the cotectics based on experimental data from Walker et al. (1979), Yang et al. (1996), Baker and Eggler (1987), Spulber and Rutherford (1983), Grove and Bryan (1983), Juster et al. (1989), Tormey et al. (1987), Kinzler and Grove (1992), Thy and Lofgren (1994), Sack et al. (1987), Bender et al. (1978) and Shi (1993).

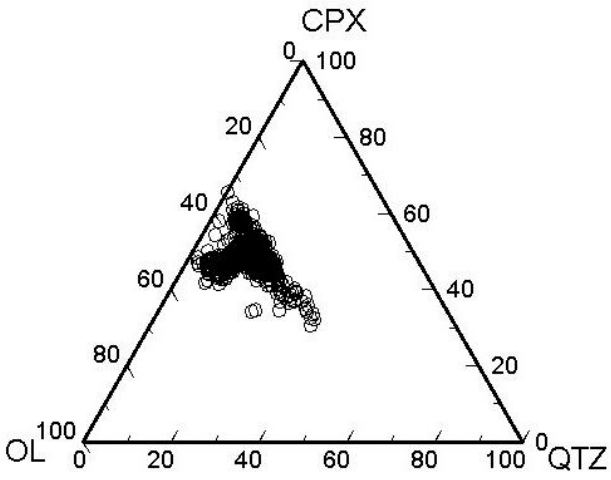

Figure 5. Melt compositions for 1110 Galapagos Volcanic glass samples.
Crystallization occurred at two different pressures. Projection method from Tormey et al., 1987.

SAMPLES

All samples used in this study to determine the pressure of crystallization are glass samples. Volcanic glass is magma that has cooled so quickly that mineral grains did not have enough time to nucleate and grow. This is important because glass analyses represent samples of quenched melts, whereas whole-rock samples may represent mixtures of crystals and melt.

Originally we downloaded 1246 glass analyses from the RIDGE data base maintained by Lamont- Doherty Earth Observatory. This data set was then filtered based on three criteria. First, after pressures were calculated for every sample we had to delete all samples that resulted in a negative pressure. Second, we deleted all samples that were not in equilibrium with olivine, plagioclase, and clinopyroxene. To do this we plotted MgO versus Al_2O_3, CaO, and CaO/ Al_2O_3 (Fig. 6 a., b., c.). Typically samples not in equilibrium had an anomalously low CaO/ Al_2O_3 ratio which indicates that no clinopyroxene was crystallizing. Finally, samples with an uncertainty level greater than 1.2 kBar for calculated pressure were deleted. The final set consisted of 1110 glasses from longitudes 84.77º W to 97.86º W. These were then sub-divided into 12 ridge segments for more detailed interpretation.

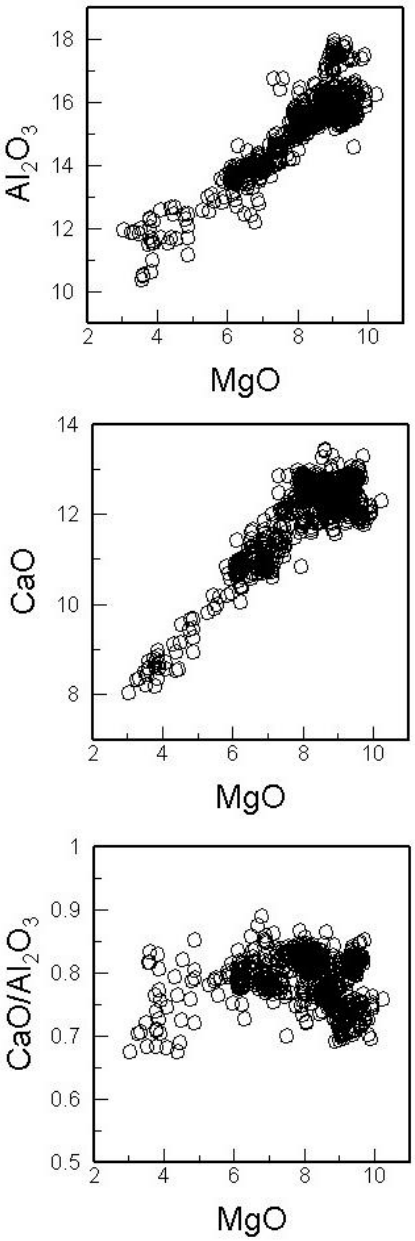

Figure 6. Plots of MgO versus Al_2O_3, CaO, and CaO/ Al_2O_3 illustrating chemical variations produced by crystallization. Variations in Al_2O_3, CaO, and CaO/ Al_2O_3 with MgO allow indentification of the mineral phases that crystallized during magma evolution.

Fig. 6a. The decrease in Al2O3 with decreasing MgO is consistent with crystallization of olivine and plagioclase.

Fig 6b. The strong decrease in CaO with decreasing MgO indicates crystallization of clinopyroxene.

Fig 6c. The nearly horizontal trend of CaO/Al2O3 with decreasing MgO indicates crystallization of clinopyroxene and plagioclase.

RESULTS

Pressures were calculated for all glasses. Below are plots of the remaining 1110 samples that had positive pressures, were in equilibrium with ol, plag, and cpx, and had uncertainties in pressure less than 1.2 kBar. Overall, results demonstrate that Galapagos magmas crystallize over a wide range of P, from 0.07 to 9.36 kBar (Fig. 7b). Not many pressures were greater than 7.0 kBar. The majority of magmas seem to have crystallized between 1 and 4 kBar. There is a slight trend that as MgO increases the pressure of crystallization increases (Fig. 7b). The calculated pressures convert to depths ranging anywhere from 0.25 to 32.93 km, but averaging near 10 km, perhaps indicating that magma crystallizes throughout the crust and upper mantle.

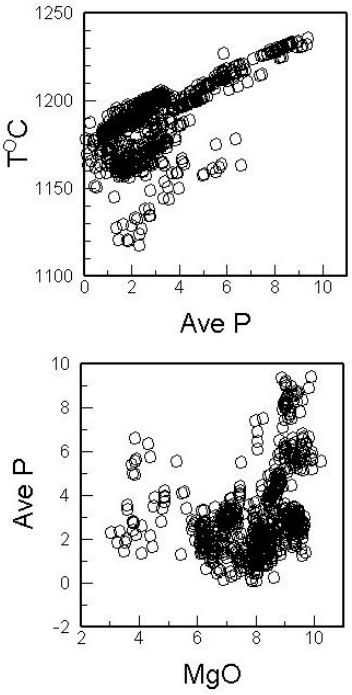

Figure 7. Summary of results obtained for all glasses excluding those considered unreliable or unrealistic.

Fig. 7a. Plot of T (ºC) calculated as described by Yang et al. (1996) versus P (GPa).

Fig. 7b. Plot of P (GPa) versus MgO.

Individual Localities

Pressures, depths, and temperature for each of the twelve locations are summarized in the appendix, Table 1. There is no strong trend in pressure of

crystallization by longitude. Also, there does not seem to be any affect on pressure of crystallization is terms of the Galapagos hot spot. We do find a wide range of crystallization at approximately 85º W and 95º W, see figure 8. This is in part due to the large amount of samples from those areas while fewer from other areas.

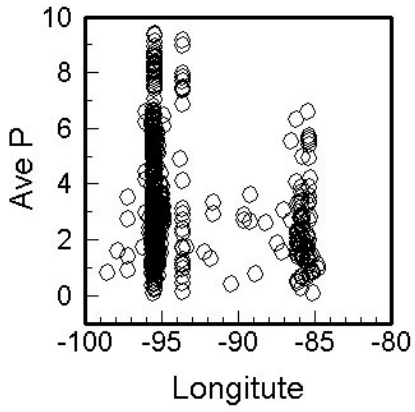

Figure 8. Pressure by Longitude. The Galapagos plume lies near 91º W

Moving east to west along the GSC we find that at approximately 95.3º W there is a transition from being a single pressure of crystallization to two distinct pressures of crystallization. This relates to the structure of magma chambers under the crust, which will be addressed in the discussion section.

DISCUSSION

Depths of Magma Chambers and Magma Pluming Systems

Recent work suggests that MORB's partially crystallize over a range of pressure from 0.001 to 1 GPa (Michael and Cornell, 1998; Herzberg, 2004). The average crustal thickness along mid-ocean ridges is 7.1±0.9 km (White et al. 1992), so that MORB crystallization must begin in the upper mantle. It seems that most Galapagos magma is crystallizing in the upper mantle. The high pressures of crystallization of up to 9.36 kBar near 94.49º W are consistent with crystallization at upper mantle depths.

We are also seeing evidence for two magma chambers west of 95.4 W, whereas only on chamber east of 95.4 W. This may be due to the thickening of the crust as you move across Galapagos plume. Detrick et al. (2004) did find evidence for plume-influenced crustal thickening out at far as 94º W.

Evidence for a single magma chamber

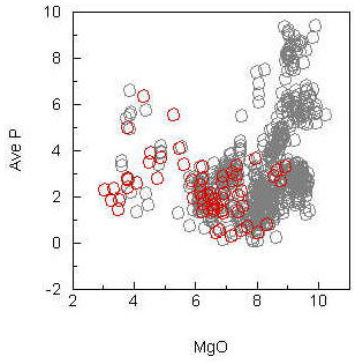

Loc. 3

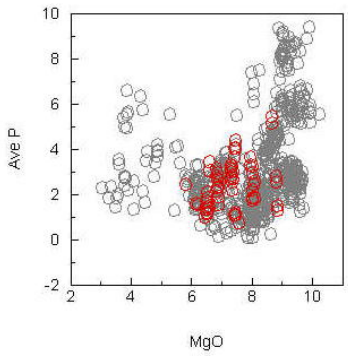

Loc. 4

Location 3 and 4, as well as others east of 95º W, seem have chambers centered around 1-3 kBar.

Evidence for two magma chambers

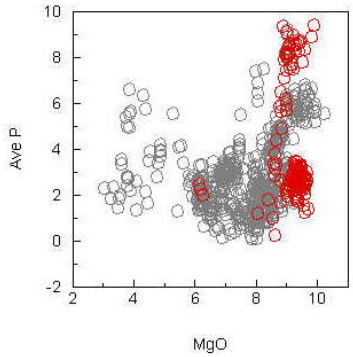

Loc. 8

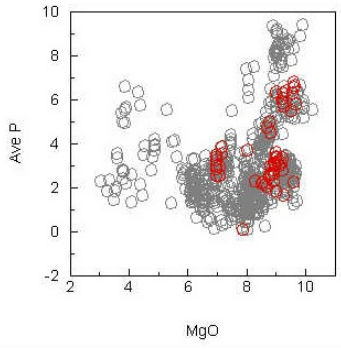

Loc. 9

Locations 8 and 9, as well as others west of 95 W, seem to have two separate magma chambers at 1-3 kBar and another at a higher pressure above 6 kBar.

Crustal Structure and Thickness

To understand the physical properties of the Galapagos ridge area seismic and geodetic studies can be consulted. Seismic studies have determined the thickness of the crust along the GSC to vary as the ridge is influence by the hot spot swell near 91.5º W. The maximum topographic swell is estimated to be ~700m (Canales et al., 2002). Coinciding with the swell Canales (2002) also finds that there is a regional mantle Bouguer anomaly (MBA) that becomes increasingly negative along the GSC toward the hot spot, with a minimum of -70 mGal at ~91.25º W. This is likely due to an increasing amount of hot, less dense magma as a result of the Galapagos plume.

Crustal thickness variations were constrained by Detrick et al. (2002) while participating in the G-PRIME experiment between 90.5º W and 98º W. They found that

west of 95º W, where a rift valley characterizes the axial morphology , crustal thickness is the thinnest (~5.6- 6 km). Between 95º W and 92.7º W, where axial morphology is transitional and displays neither an axial valley nor a topographic high, crustal thickness is 6-7 km and the top of an axial magma chamber is at depths of 2.5-4.25 km. East of 92.7º W, where the GSC is associated with an axial high, the crust is 7-8 km thick and the top of an axial magma chamber is only ~1.38- 2.25 km. There is significant thickening of ~2.3 km east of 94º W (from 5.6 to 7.9 km) indicating that the primary effect of the hot spot on melt productivity beneath the GSC is confined to a distance less than ~400 km from the center of the hot spot (Detrick et al., 2002).

The minimum depth of magma chamber, using our method, is 0.23 km, while most depths are greater than 8 km. This requires that magma chambers are ponding at the base of the crust, but that there are also magma chambers throughout the crust.

Fracture Zones and Spreading Rate

Herzberg et al. (2004) found that fast- and intermediate- spreading centers exhibit more than 50% of MORB glass compositions showing evidence of ol+plag+cpx fractionation at crustal pressures ranging from 1 atm to 0.2 GPa. The remainder of samples showing fractionation at pressures of 0.2- 1.0 GPa. Shallow depth olivine gabbro fractionation is prominent among MORB from the East Pacific Rise and Juan de Fuca Ridge, as well as the Galapagos Spreading Center. These results are consistent with models of layered gabbro formation (i.e. layer 3) in steady-state magma chambers below fast-spreading ridges (Herzberg, 2004). MORB glasses from slow-spreading centers

indicate pressures of crystallization that correspond to mantle depths. In general, fracture zones are usually associated with high pressures of crystallization (Herzberg, 2004).

CONCLUSIONS

The average magma chamber depth is ~10±2.5 km. This depth is within the upper mantle, suggesting the magma pools and begins to crystallize at the base of the crust. There is evidence for single magma chambers east of 95 W and multiple magma chambers west of 95 W, presumably associated with the difference in crustal thickness due to the plume. The Galapagos plume is not showing a strong effect on the depth of magma chambers, but is showing some geochemical effects that need to be further examined.

REFERENCES

Canales, J. P., J. J. Danobeitia, R. S. Detrick, E. E. E. Hooft, R. Bartolome, and D. Naar, Variations in axial morphology along the Galapagos Spreading Center and the influence of the Galapagos hot spot, *J. Geophys. Res., 102*, 27,341- 27,354, 1997.

Canales, J. P., G. Ito, R. Detrick, and J. Stinton, Crustal thickness along the western Galapagos spreading center and the compensation of the Galapagos hotspot swell, *Earth Planet. Sci Lett.*, 203, 311-327, 2002.

Detrick et al. Correlated geophysical and volcanological manifestations of plume-ridge interaction along the Galapagos Spreading Center. *Geochemistry, Geophysics, and Geosystems,* 3, 10, 2002.

.

Fisk, M. R., A. E. Bence, and J. -G. Schilling, Major element chemistry of Galapagos Rift zone magmas and their phenocrysts, *Earth Planet. Sci. Lett., 61*, 171-189, 1982.

Grove , T.L., Kinzler, R.J. & Bryan, W.B. Fractionation of mid-ocean ridge basalt (MORB). *Am. Geophys. Union Geophys. Monogr.* 71,281-310, 1992.

Herzberg, C., Herzberg, C., prefacer & Wilson, M., prefacer. (2004) Partial Crystallization of mid-ocean ridge basalts in the crust and mantle, *J. Petrol*. 45, 2389-2405.

Hey, R. N., Tectonic evolution of the Cocos-Nazaca spreading center, *Geol. Soc. Am. Bull, 88*, 1404- 1420, 1977.

Ito, G., and J. Lin, Oceanic Spreading center-hot spot interactions: Constraints from along-isochron bathymetric and gravity anomalies, *Geology, 7*, 657- 660, 1995a.

Kelley, Daniel and Michael Barton, Pressures of crystallization of Icelandic magmas, *J. Petrol*, 2008.

Klein, Emily M and C. Langmuir, Global correlations of ocean ridge basalt chemistry with axial depth and crustal thickness, *J. Geophys. Res.*, 92, 8089-8115, 1987.

McBirney, A.R., H. Williams. Geology and Petrology of the Galapagos Islands, *The Geological Society of America, Inc. Memoir 118.* 7- 1969.

Michael, P.J. & Cornell, W.C. Influence of spreading rate and magma supply on crystallization and assimilation beneath mid-ocean ridges; evidence from chlorine and major element chemistry of mid-ocean ridge basalts. *J. Geophys. Res., B, Solid Earth and Planets* 103, 18, 325-18, 356, 1998.

O'Hara, M.J., Are ocean floor basalts primary magma?, *Nature (London)* 220, 683-686, 1986.

Schilling, J.-G., R. N. Anderson, and P. Vogt, Rare earth, Fe and Ti variations along the Galapagos Spreading Center and their relationship to the Galapagos Mantle Plume, *Nature, 261*, 108- 113, 1976.

Sturkell, E, et al, Volcano geodesy and magma dynamics in Iceland. *J. Volcanol. Geotherm Res.*, 150,14-34, 2006.

Toomey, D. R., E. E. E. Hooft, S. Solomon, D. James, and M. Hall, Upper mantle structure beneath the Galapagos archipelago from body wave data, *Eos Trans. AGU, 82*(46), Fall Meet. Suppl., F1205, 2001.

Tormey, D. R., Grove, T. L. & Bryan, W. B., Experimental petrology of normal MORB near the Kane Fracture Zone: 22°–25°N, Mid-Atlantic Ridge. *Contributions to Mineralogy and Petrology* 96, 121–139, 1987.

Verma, S. P., and J.-G. Schilling, Galapagos hot spot-spreading center system, 2, $^{87}Sr/^{86}Sr$ and large ion lithophile element variations (85º W- 101º W), *J. Geophys. Res., 87*, 10,838- 10,856, 1982.

Verma S.P., J.-G. Schilling, and D.G. Waggoner, Neodymium isotopic evidence for Galapagos hot spot- spreading sentre system evolution, *Nature, 306,* 654-657, 1983.

Walker, D., DeLong, S.E. & Shibata, T. Abyssal tholeiites from the Oceanograper fracture zone; II, Phase equilibria and mixing. *Contribition to Mineralogy and Petrology,* 70, 111-125, 1979.

White R.S., McKenzie, D. & O'Nions, R.K, Oceanic crustal thickness from seismic measurements are rare earth element inversions. *J. Geophys. Res., B, Solid Earth and Planets,* 97, 19, 683-19, 715, 1992.

White, W.M., A.R. McBirney, and R.A. Duncan, Petrology and geochemistry of the Galapagos Islands: Portrait of a pathological mantle plume, *J. Geophys. Res., 98* 19,533-19,563, 1993.

White, W.M. Galapagos geology on the web; a brief introduction to the geology of the Galapagos, http://www.geo.cornell.edu/geology/GalapagosWWW/Galapagos Geology.html, 2007

Wilson D.S., and R.N. Hey, History of rift propagation and magnetization intensity for the Cocos-Nazaca spreading center, *J. Geophys. Res., 100*, 10,041- 10,056, 1995.

Yang, H. J., Grove, T. L. & Kinzler, R. J, Experiments and models of anhydrous, basaltic olivine-plagioclase-augite saturated melts from 0.001-10 kbar. *Contributions to Mineralogy and Petrology*,124, 1-18, 1996.

APPENDIX

Table 1. Summary of Calculated Pressures, Depths, and Temperatures

	Locality	n	Ave P	Max	Min	Depth (km)	Ave T	Max	Min
1	84.77 to 85.57ºW	44	2.32 ± 1.62	6.58	0.07	8.16	1161.5 ± 17.7	1191.4	1126.95
2	85.83 to 92.23ºW	68	2.32 ± 1.15	6.33	0.28	8.16	1162.9 ± 18.9	1201.1	1117.5
3	93.3 to 94.97ºW	59	3.51 ± 2.68	9.16	0.14	12.35	1190.3 ± 21.7	1233.2	1161.5
4	95.0 to 95.3ºW	72	2.34 ± 0.97	5.41	0.74	8.23	1177.5 ± 11.5	1209.2	1157.3
5	95.3 to 95.37ºW	97	2.29 ± 1.25	5.9	0.64	8.06	1186.9 ± 9.7	1213.5	1157.3
6	95.42 to 95.44ºW	62	3.29 ± 1.79	8.32	0.66	11.58	1170.7 ± 16.7	1224.8	1158.5
7	95.47ºW	282	2.15 ± 1.23	5.13	0.19	7.57	1183.4 ± 12.5	1202.5	1156.6
8	95.493 to 95.497ºW	241	3.87 ± 2.4	9.36	0.24	13.62	1204.8 ± 14.3	1235.3	1160.5
9	95.51 to 95.537ºW	59	3.65 ± 1.58	6.75	0.09	12.84	1198.9 ± 14.3	1226.5	1169
10	95.55ºW	84	4.77 ± 1.32	6.61	1.69	16.78	1203.4 ± 13.4	1216.7	1169.4
11	95.62 to 95.78ºW	29	2.23 ± 1.72	6.2	0.37	7.85	1185.4 ± 14.6	1215.4	1149.6
12	96.01 to 97.86ºW	12	3.14 ± 1.9	6.58	0.92	11.05	1185.6 ± 19.3	1217.1	1162.4
ALL	84.77 to 97.86ºW	1110	2.99 ± 1.92	9.36	0.07	10.52	1188.4 ± 19.4	1235.3	1117.45